

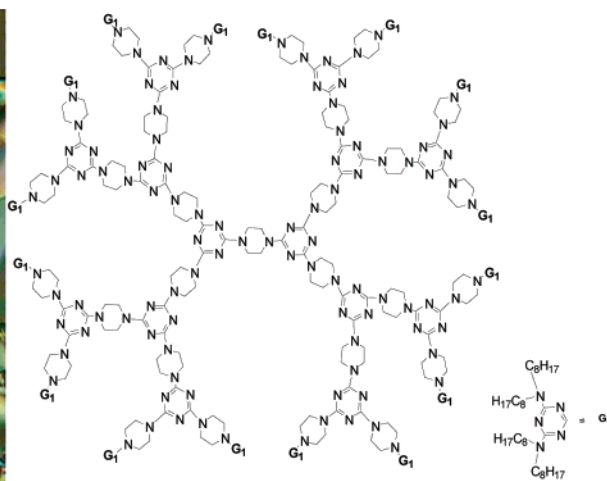
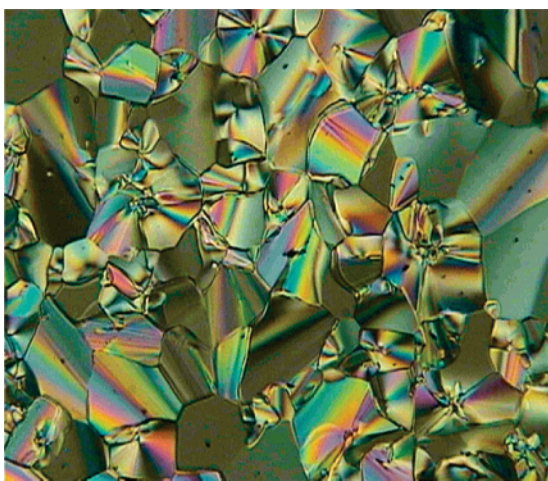
Star-Shaped Mesogens of Triazine-Based Dendrons and Dendrimers as Unconventional Columnar Liquid Crystals

Long-Li Lai,^{*,†} Cheng-Hua Lee,[†] Ling-Yung Wang,[†] Kung-Lung Cheng,[‡] and Hsiu-Fu Hsu[§]

Department of Applied Chemistry, National Chi Nan University, Puli, Nantou, Taiwan 545, Applied Chemistry Division, Material and Chemical Research Laboratories, Industrial Research Institute, Hsinchu, Taiwan 300, and Department of Chemistry, Tamkang University, Tamsui, Taiwan 251

lilai@ncnu.edu.tw

Received September 10, 2007



Dendrons $G_n\text{-Cl}$ and $G_n\text{-NH}$ ($n = 2-4$) and novel dendrimers $G_n\text{-N}\sim\text{N}\text{-}G_n$ ($n = 2-4$) based on triazine and piperazine units were efficiently prepared in good yields without employing the protection and deprotection processes and are fully characterized by ^1H NMR and ^{13}C NMR spectroscopies, elemental analysis, and mass spectroscopy. These compounds are transparent and possess good thermal stability. $G_4\text{-Cl}$ shows a monotropic columnar phase in a narrow range with a coexisting crystalline phase. Dendron $G_4\text{-NH}$ shows a rectangular column-phase, and dendrimer $G_4\text{-N}\sim\text{N}\text{-}G_4$ exhibits a monotropic hexagonal columnar phase. These identifications were supported by the polarizing optical scope and powder XRD studies.

Introduction

Dendrons and dendrimers, often containing central cores, bridging units, and terminal functionalities, are branchlike molecules and therefore possess three-dimensional or branched structures. They have unusual properties such as multiple functionality and monomolecular weight and have been extensively investigated in recent years.¹ Particularly, star-shaped mesogens of dendrons or dendrimers have attracted much attention owing to their easy governing of morphology by the

thermal process, during which columnar mesophases are formed via the self-assembly.²⁻⁴ Generally, dendritic mesogens consist of rigid centers, flexible spacers, and peripheral mesogenic units as described in the literature.³ However, star-shaped mesogens containing central rigid cores and flexible peripheral chains, which may be regarded as being unconventional, are noteworthy, as their morphology is formed by restricted conformational freedom, potentially allowing such molecules to form cavities,

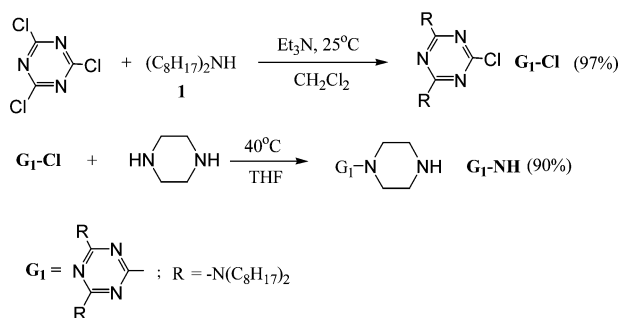
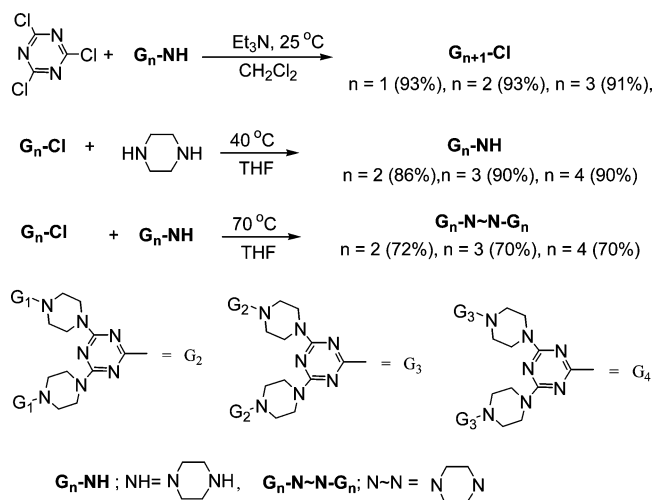
(2) (a) Chang, T. H.; Wu, B. R.; Chiang, M. Y.; Liao, S. C.; Ong, C. W.; Hsu, H. F.; Lin, S. Y. *Org. Lett.* **2005**, *7*, 4078. (b) Foster, E. J.; Babuin, J.; Nguyen, N.; Williams, V. E. *Chem. Commun.* **2004**, 2052. (c) Lehmann, M.; Gearba, R. I.; Koch, M. H. J.; Ivanov, D. A. *Chem. Mater.* **2004**, *16*, 374. (d) Simpson, C. D.; Wu, J.; Watson, M. D.; Müllen, K. *Chem. Commun.* **2004**, 494. (e) Ong, C. W.; Liao, S. C.; Chang, T. H.; Hsu, H. F. *J. Org. Chem.* **2004**, *69*, 3181.

[†] National Chi Nan University.

[‡] Industrial Research Institute.

[§] Tamkang University.

(1) Newkome, G. R.; Moorefield, C. N.; Vögtle, F. *Dendrimers and Dendrons*; Wiley-VCH: Weinheim, 2000.

SCHEME 1. Preparation of Compounds $G_1\text{-Cl}$ and $G_1\text{-NH}$ SCHEME 2. Preparation of Compounds $G_n\text{-Cl}$, $G_n\text{-NH}$ and $G_n\text{-N}\sim\text{N}\sim G_n$ 

where guest molecules can be incorporated.⁴ Additionally, functional mesogens self-assembled into columnar phases have been targeted as candidates for various devices such as photovoltaics, LEDs, and sensors, depending on their corresponding molecular structures and macroscopic properties.^{5,6} Although many *N*-heterocyclic unconventional mesogens self-assembled into columnar phases have been recently investigated,² to our best knowledge, only a few *N*-heterocyclic unconventional mesogens of high-generation dendrons or dendrimers ($n \geq 4$) assembled into columnar phases are reported so far.⁴

Recently, we have preliminarily reported a convenient method to prepare dendrons, i.e., $G_n\text{-Cl}$ and $G_n\text{-NH}$ ($n = 1-4$) (Schemes 1 and 2) without employing protection and depro-

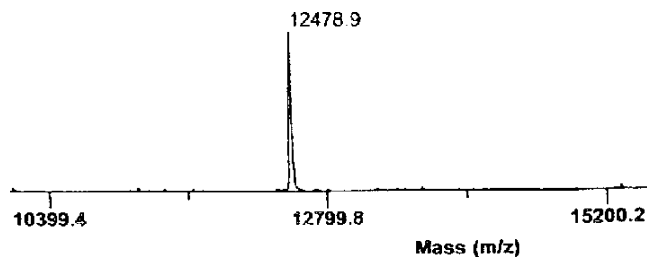


FIGURE 1. Mass spectrum of $G_4\text{-N}\sim\text{N}\sim G_4$.

tection processes, and the yield of the dendron for each generation is excellent.⁷ In other words, the characteristics of easy preparation and purification allow us to consider the potential applications of their derivatives. We thus further prepare their corresponding dendrimers $G_n\text{-N}\sim\text{N}\sim G_n$ ($n = 2-4$; Scheme 2) and investigate their mesogenic phases and other physical properties. It is well-known that conventional dendrimers potentially function as catalytic materials,⁸ molecular micelles,⁹ light-harvesting molecules,¹⁰ drug-transporting agents,¹¹ and porous and interfacial materials.^{12,13} The unconventional dendrons or dendrimers exhibiting mesogenic behaviors may have the new applications in addition to their corresponding utilities. We thus investigate the mesogenic phases of dendrons $G_n\text{-Cl}$ and $G_n\text{-NH}$ ($n = 3, 4$) and dendrimers $G_n\text{-N}\sim\text{N}\sim G_n$ ($n = 2-4$). Compounds $G_4\text{-Cl}$, $G_4\text{-NH}$, and $G_4\text{-N}\sim\text{N}\sim G_4$ all exhibit columnar phases during the thermal process, and now we report all these results.

Results and Discussion

Nucleophilic substitution of *N*-heterocycles is a major topic in heterocyclic chemistry, and the reactivity of the heteroaromatics is significantly influenced by the substituents. Therefore, as reported by Simanek and Takagi,¹⁴ it is possible to allow two or three equivalents of amines to react with cyanuric chloride at controlled conditions, because the amino moieties can enrich the electron density of the heteroaromatics and subsequently disfavor the nucleophilic substitution. In the presence of triethylamine, 2.2 equiv of the diluted dioctylamine **1** in CH_2Cl_2 was added to the diluted cyanuric chloride in CH_2Cl_2 in an ice bath for 1 h and then stirred at room temperature for 24 h. Five equivalents of KOH (based on cyanuric chloride) in water was then added, and the resulting solution was extracted with CH_2Cl_2 and then concentrated at reduced pressure to give

(7) Lai, L. L.; Wang, L. Y.; Lee, C. H.; Lin, Y. C.; Cheng, K. L. *Org. Lett.* **2006**, *8*, 1541.

(8) (a) Knapen, J. W. J.; van der Made, A. W.; de Wilde, J. C.; van Leeuwen, P. W. N. M.; Wijkens, P.; Grove, D. M.; van Koten, G. *Nature* **1994**, *372*, 659. (b) Reynhardt, J. P. K.; Yang, Y.; Sayari, A.; Apler, H. *Chem. Mater.* **2004**, *16*, 4095.

(9) (a) Jansen, J. F. G. A.; de Brabander-van den Berg, E. M. M.; Meijer, E. W. *Science* **1994**, *266*, 1226. (b) Hawker, C. J.; Frechet, J. M. J. *J. Chem. Soc., Perkin Trans. 1* **1992**, 2459.

(10) Jiang, D. L.; Aida, T. *Nature* **1997**, *388*, 1681.

(11) (a) Haensler, J.; Szoka, F. C., Jr. *Bioconjugate Chem.* **1993**, *4*, 372. (b) Tang, M. X.; Redemann, C. T.; Szoka, F. C., Jr. *Bioconjugate Chem.* **1996**, *7*, 703.

(12) Landskron, K.; Ozin, G. A. *Science* **2004**, *306*, 1529.

(13) Garcia-Martinez, J. C.; Scott, R. W. J.; Crooks, R. M. *J. Am. Chem. Soc.* **2003**, *125*, 11190.

(14) (a) Zhang, W.; Simanek, E. E. *Org. Lett.* **2000**, *2*, 843. (b) Takagi, K.; Hattori, T.; Kunisada, H.; Yuki, Y. *J. Polym. Sci., Part A: Polym. Chem.* **2000**, *38*, 4385. (c) Schnabel, W. J.; Rätz, R.; Kober, E. *J. Org. Chem.* **1962**, *27*, 2514. (d) Thurston, J. T.; Dudley, J. R.; Kaiser, D. W.; Hechenbleikner, I.; Schaefer, F. C.; Holm-Hansen, D. *J. Am. Chem. Soc.* **1951**, *73*, 2981.

(3) (a) Saez, I. M.; Goodby, J. W. *J. Mater. Chem.* **2005**, *17*, 4979 and references cited therein. (b) McKenna, M. D.; Barbera, J.; Marcos, M.; Serrano, J. L. *J. Am. Chem. Soc.* **2005**, *127*, 619. (c) Zeng, X.; Ungar, G.; Liu, Y.; Percec, V.; Dulcey A.; Hobbs, J. K. *Nature* **2004**, *428*, 157. (d) Ungar, G.; Liu, Y.; Zeng, X.; Percec, V.; Cho, W.-D. *Science* **2003**, *299*, 1208. (e) Singer, S. K. D.; Percec, V.; Bera, T. K.; Miura, Y.; Glodde, M. *Phys. Rev. B* **2003**, *76*, 1.

(4) (a) Bertrand, B.; Guillon, D. *Adv. Polym. Sci.* **2006**, *201*, 45. (b) Tschierske, C. *Annu. Rep. Prog. Chem., Sect. C: Phys. Chem.* **2001**, *97*, 191 and references therein. (c) Kato, T.; Mizoshita, N.; Kishimoto, K. *Angew. Chem., Int. Ed.* **2006**, *45*, 38 and references therein. (d) Grafe, A.; Janietz, D.; Frese, T.; Wendroff, J. H. *Chem. Mater.* **2005**, *17*, 49789. (e) Meier, H.; Lehmann, M.; Kolb, U. *Chem. Eur. J.* **2000**, *6*, 2462.

(5) (a) Schmidt-Mende, L.; Fechtenkotter, A.; Müllen, K.; Moons, E.; Friend, R. H.; MacKenzie, J. D. *Science* **2001**, *293*, 1119. (b) Freudenmann, R.; Behnisch, B.; Hanack, M. *J. Mater. Chem.* **2001**, *11*, 1618. (c) Boden, N.; Bushby, R. J.; Clements, J.; Movaghgar, B. *J. Mater. Chem.* **1999**, *9*, 2081.

(6) Foster, E. J.; Lavigueur, C.; Ke, Y. C.; Williams, V. E. *J. Mater. Chem.* **2005**, *15*, 4062.

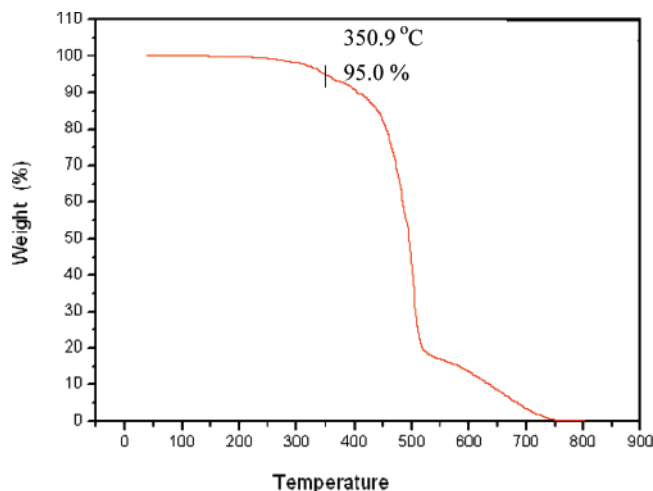


FIGURE 2. Decomposition of $G_3-N\sim N-G_3$ under nitrogen by TGA.

TABLE 1. Phase Transition Temperature and Corresponding Enthalpies (kJ/mol), in Parentheses, of the Dendrons and Dendrimers^c

$G_2-N\sim N-G_2$	K	$\xrightarrow{131.5(107.7)}$	I
		$\xleftarrow{112.6, 116.5 (-100.4)^a}$	
$G_3-N\sim N-G_3$	K	$\xrightarrow{128.2, 132.7 (171.4)^a}$	I
		$\xleftarrow{97.6 (-163.5)}$	
$G_4-N\sim N-G_4$	K	$\xrightarrow{175.4 (38.7)}$	I
		$\xleftarrow{143.3 (-22.5) \text{ Col}_h \quad 160.0 (-6.2)}$	
G_3-NH	K	$\xrightarrow{125.7 (11.6)}$	K ₁
		$\xleftarrow{108.1 (-17.1)}$	
		$\xrightarrow{149.5 (51.4)}$	I
		$\xleftarrow{135.6 (-36.1)}$	
G_4-NH	K	$\xrightarrow{132.9(15.1)}$	Col _r
		$\xleftarrow{113.6 (-10.7)}$	
		$\xrightarrow{163.7 (33.9)}$	I
		$\xleftarrow{158.0 (-6.9)}$	
G_3-Cl	K	$\xrightarrow{128.1 (4.8)}$	K ₁
		$\xleftarrow{108.7 (-63.8)}$	
		$\xrightarrow{137.7 (72.5)}$	I
		$\xleftarrow{108.7 (-63.8)}$	
G_4-Cl	K	$\xrightarrow{179.5(48.0)}$	I
		$\xleftarrow{158.8 (-21.2) \text{ Col} \quad -167.6 (-8.1)}$	

^a Peaks overlapped ^b The transition temperature and corresponding enthalpies were recorded at the second cycles between the isotropic and room temperatures. ^c Abbreviations: K, K₁ = crystalline, Col = columnar phase, Col_h = hexagonal columnar phase, Col_r = rectangular columnar phase, I = isotropic liquid.

G_1-Cl which was isolated in 97% yield after chromatography. It is worthwhile to point out that diluted reagents and a large excess of KOH have to be used in the corresponding reaction and workup processes, respectively, to avoid vigorous reaction and to completely remove HCl produced in the course of reaction. Subsequently, 3 equiv of piperazine in THF were allowed to react with G_1-Cl in THF at 40 °C for 20 h, while the amine-salt had precipitated. Analogously, 5 equiv of KOH in water were then added, and compound G_1-NH was subsequently obtained in 90% yield after workup and chromatogra-

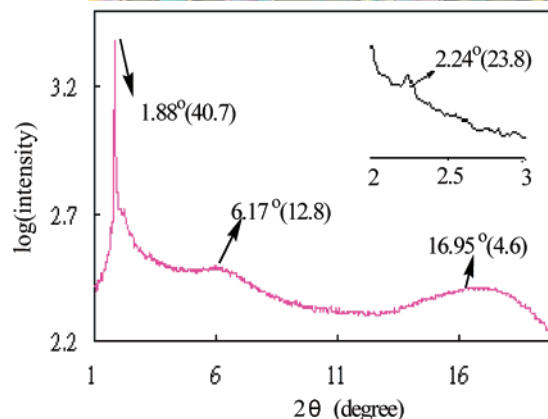
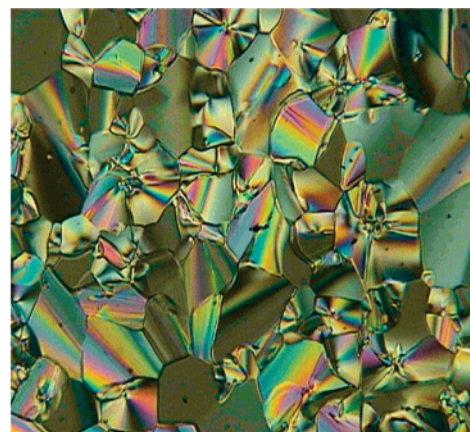


FIGURE 3. Optical texture of $G_4-N\sim N-G_4$ at 159 °C (top) and the XRD pattern of $G_4-N\sim N-G_4$ at 150 °C (bottom).

phy. It is surprising to find that no disubstituted product ($G_1-N\sim N-G_1$) could be detected after workup. We believe that this may arise from the transannular effect of piperazine¹⁵ or from the steric effect of the dioctyl moieties (Scheme 1).

Similarly, an excess of compound G_1-NH was also treated with cyanuric chloride in the presence of triethylamine, and G_2-Cl was obtained accordingly, which further gave G_2-NH in a similar manner as described in the preparation of G_1-Cl and G_1-NH . G_2-Cl and G_2-NH reacted in THF at 70 °C for 20 h and then were washed with 10 equiv of aqueous KOH solution to give $G_2-N\sim N-G_2$ in ~70% yield after chromatography. Analogously, compounds G_3-Cl , G_3-NH , $G_3-N\sim N-G_3$, G_4-Cl , G_4-NH , and $G_4-N\sim N-G_4$ were prepared in good yields by alternatively incorporating triazine and piperazine functionalities on repeating the previous procedures (Scheme 2). It is noteworthy that there were no protecting and deprotecting processes involved during the preparation of the dendrons G_n-Cl and G_n-NH ($n = 1-4$). Also, all the reactions were carried out in mild conditions, and no specially dried solvents were needed, as the reactivity of the amine is much higher than that of water, and a small amount of the moisture in the solvent did not obviously affect the reaction results. Compounds $G_n-N\sim N-G_n$ ($n = 2-4$) were characterized by ¹H and ¹³C NMR spectroscopies, elemental analysis, and mass spectroscopy. The mass spectrum of $G_4-N\sim N-G_4$, obtained by MALDI-TOF technique, is illustrated in Figure 1, and a peak at 12478.9 arising from the

(15) (a) Lai, L. L.; Wang, E.; Luh, B. J. *Synthesis* **2001**, 3, 361. (b) Wang, T.; Zhang, Z.; Meanwell, N. A. *J. Org. Chem.* **1999**, 64, 7661. (c) Chou, W. C.; Tan, C. W.; Chen, S. F.; Ku, H. *J. Org. Chem.* **1998**, 63, 10015.

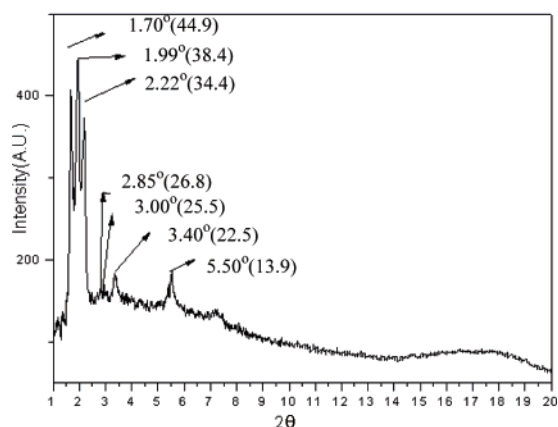
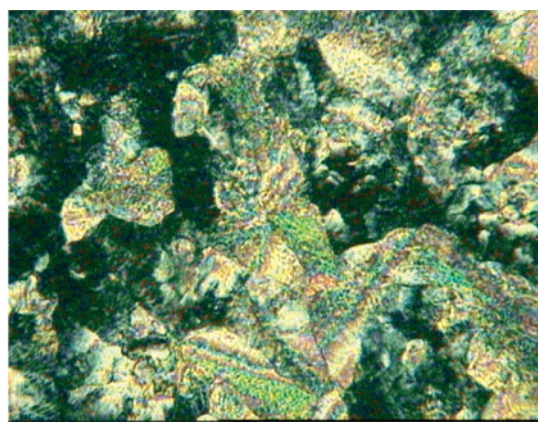


FIGURE 4. Texture of crystal of $G_4-N\sim N-G_4$ at room temperature (top) and the XRD pattern of $G_4-N\sim N-G_4$ at room temperature (bottom).

$(M + H)^+$ ions was observed. $G_4-N\sim N-G_4$ was further characterized by microanalysis, and the errors for calculated and experimental percentages for C, H, and N are within 0.4%.

To understand the optical property of the dendrimers, $G_3-N\sim N-G_3$ in CH_2Cl_2 representing this series of molecules, was also investigated by UV spectroscopy. No significant absorbance beyond 280 nm was observed in the UV-vis spectrum, which is important in the application of optical films. The thermal stability of compound $G_3-N\sim N-G_3$ was also investigated by TGA under nitrogen, and this compound is reasonably stable and starts to decompose at $\sim 300^\circ C$ (Figure 2).

The liquid crystalline properties of G_n-Cl , G_n-NH ($n = 3, 4$) and $G_n-N\sim N-G_n$ ($n = 2-4$) are summarized in Table 1. For all these compounds, no thermal decomposition was observed during the thermal processes. It is interesting to note that, for these dendrons or dendrimers, the super-cooling phenomena of the higher generations are not more serious than those of lower generations.

Dendrimers $G_2-N\sim N-G_2$ and $G_3-N\sim N-G_3$ do not show any liquid crystalline phase. However, $G_4-N\sim N-G_4$ does exhibit a monotropic columnar phase characterized by a mosaic texture (Figure 3, top) with a $\sim 17^\circ$ range upon cooling. This columnar phase was further investigated by powder-XRD study (Figure 3, bottom). The wide-angle signal at 4.6 \AA is attributed to the liquidlike correlation of the molten chains. A broad signal at 12.8 \AA is assigned to the intracolumnar stacking distance. A sharp peak in the small-angle region corresponding to a d -spacing of 40.7 \AA and a weak signal at 23.8 \AA were indexed as 10 and 11, respectively, for hexagonally arranged columns.

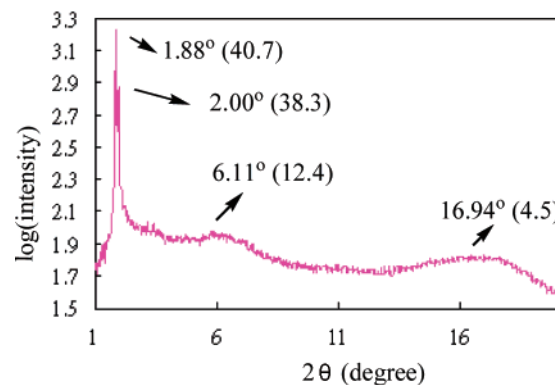
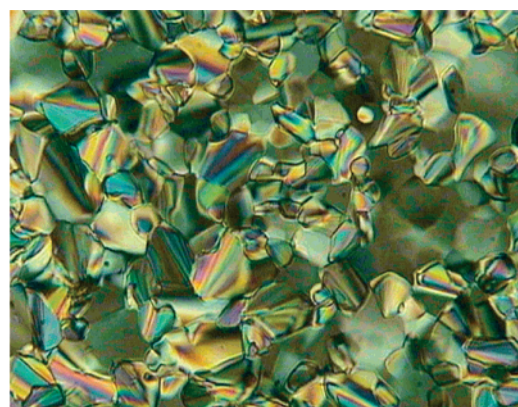


FIGURE 5. Optical texture of G_4-NH at $158^\circ C$ (top) and the XRD pattern of G_4-NH at $150^\circ C$ (bottom).

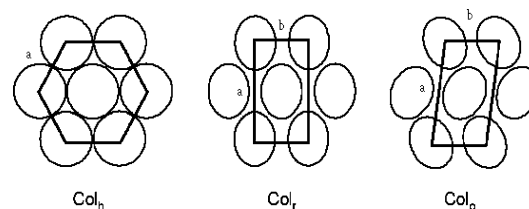


FIGURE 6. Schematic representation of the 2D lattices of columnar hexagonal (Col_h), columnar rectangular (Col_r), and columnar oblique (Col_o) phases

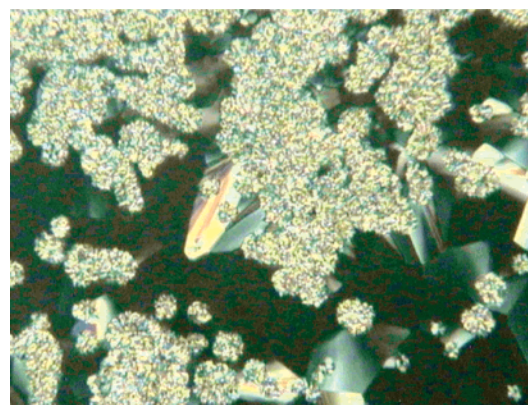


FIGURE 7. Optical texture of G_4-Cl at $160^\circ C$ showing coexistence of columnar and crystalline phases.

Accordingly, the number of molecules in a unit cell, Z , was calculated to be approximately 1 (0.89), assuming the density is equal to 1 g cm^{-3} and the hexagonal lattice constant and the mean stacking distance within columns obtained from powder

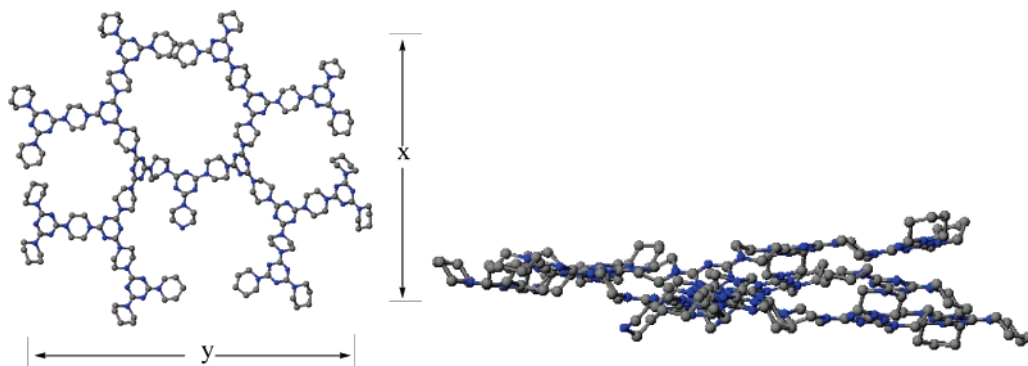


FIGURE 8. Optimized conformation of **G₄-NH** at gas phase by an MM2 model in CaChe program (left) and a side-view of **G₄-NH** (right) (hydrogens are omitted for clarity, C: gray, N: blue).

XRD studies are 40.7 and 12.8 Å, respectively.¹⁶ However, the low intensity of the mid-angle signal that may have arisen from the unaligned sample does not allow the unambiguous assignment. A slight enhancement of the 11 signal can be obtained when the intensity is in a logarithmic scale. With uncertainty about the 11 signal and in the absence of other reflections, an oblique phase cannot be excluded. On cooling to room temperature, a new texture and a new XRD pattern indicative of a phase of crystal are demonstrated in Figure 4.

Dendron **G₃-NH** does not show any liquid crystalline phases during thermal processes. However, dendron **G₄-NH** shows a columnar phase, as evidenced by its mosaic texture under polarizing optical microscope (Figure 5, top). The mesogenic range for **G₄-NH** is found to be about 30° in the heating process. The identity of the columnar phase of **G₄-NH** was further studied by powder XRD (Figure 5, bottom). Two sharp peaks were detected in the small-angle region pointing to a rectangular columnar phase although no other reflections can be observed to assign the *C*₂ or *P*₂ space group symmetries, probably again due to the unaligned nature of the sample. Lattice constants of *a* and *b* are calculated to be 81.4 Å and 43.3 Å based on *d*-spacings of 40.7 and 38.3 Å for 20 and 11 reflections, respectively (Figure 6). A broad signal at 12.4 Å is assigned to the mean stacking distance within columns. The wide-angle signal at 4.5 Å is attributed to the liquidlike correlation of the molten chains. Accordingly, the number of molecules in a unit cell, *Z*, was calculated approximately to be 2 (1.85), assuming the density is equal to 1 g cm⁻³ and the rectangular lattice constants and the mean stacking distance within columns obtained from powder XRD studies are 40.7 Å, 38.3 Å, and 12.4 Å, respectively.¹⁷ On the other hand, dendron **G₃-CI** does not show any liquid crystalline phases during thermal processes. Dendron **G₄-CI** shows a columnar phase, coexisting with a crystalline phase with a temperature range of ~9° only in the

cooling process. Under the polarizing optical microscope, **G₄-CI** exhibits a columnar phase first, and then the percentage of the crystalline phase increases quickly (Figure 7).

For better understanding on the molecular conformation of the dendrons and dendrimers, simulations were carried out by CaChe program using MM2 model at gas phase. Topologies of the central rigid cores of the dendrons and dendrimers were the focus of simulations because the various topology of each dendron and dendrimer should provide useful information to justify their corresponding molecular conformation. For simplicity, the piperidine moiety was used to replace the dioctylamine moiety in the process of optimization. The starting conformation of **G₁-CI** (R = piperidine) was first established by combination of one planar triazine and two piperidine moieties in chair form and then optimized. The conformation of **G₁-NH** (R = piperidine) was then obtained by combination of the optimized **G₁-CI** (R = piperidine) with piperazine in chair form and then optimized. Similarly, the conformation of **G₂-CI** (R = piperidine) was obtained by combination of the planar triazine with two optimized **G₁-NH** units (R = piperidine) and then optimized. Accordingly, the optimized conformations of **G₄-CI** and **G₄-NH** (R = piperidine) were thus obtained, respectively. The conformation of **G₄-N~N-G₄** (R = piperidine) is obtained by combination of the optimized **G₄-CI** and **G₄-NH** and then optimized.

The optimized conformation of **G₄-NH** (Figure 8, R = piperidine; left) shows an elliptical shape, and its length *x* and width *y* (*x* and *y*; measured from the corresponding nitrogens of the triazine moieties) were measured to be ~38.4 Å and 32.6 Å, respectively. A side view of the optimized structure shows the core is slightly helical (Figure 8, right). After optimizing **G₄-CI** (R = piperidine), a conformation similar to that of **G₄-NH** was also obtained. However, it is interesting to note that **G₄-NH** possesses a rectangular columnar phase during thermal processes, while **G₄-CI** does not behave correspondingly. It is thus believed that the formation of a rectangular columnar phase for **G₄-NH** is due to the intermolecular H-bond interaction between H and N atoms of the piperazine unit.

The optimized conformation of **G₄-N~N-G₄** (Figure 9, R = piperidine; left) shows a relatively circular shape and its length *x* and width *y* (*x* and *y*; measured from the corresponding nitrogens of the triazine moieties) were measured to be ~40.4 Å and 42.8 Å, respectively. Compared with **G₄-NH**, **G₄-N~N-G₄** shows a smaller difference between *x* and *y* and thus is regarded to be more nonelliptical. From XRD studies, the more circular **G₄-N~N-G₄** thus shows a hexagonal arrangement of

(16) For a hexagonal lattice, the relationship between density, ρ , and number of molecules in a unit cell, Z , is given by: $\rho = (M/N)/(V/Z)$, where M is the molar mass (g), N is Avogadro's number, and V is the unit cell volume (cm³). From the above equation, Z can be deduced as $Z = (\rho VN)/M = (\rho(\sqrt{3}/2)a^2c \times 10^{-24})N/M$, where a is the hexagonal lattice constant, c is the mean stacking distance within columns. Assuming the density equals 1 g cm⁻³, the number of molecules in a unit cell Z for the columnar hexagonal phase of **G₄-N~N-G₄** is calculated to be close to 1 (0.89) ($\rho = 1$; $a = 40.7$ Å; $c = 12.8$ Å; $M: 12477$; $N: 6.02 \times 10^{23}$).

(17) For a rectangular lattice, the equation is deduced as: $Z = (\rho abc \times 10^{-24})N/M$, where a and b are lattice constants of the rectangular phase. Assuming the density equals to 1 g cm⁻³, the number of molecules in a unit cell Z for the columnar rectangular phase of **G₄-NH** is calculated to be close to 2 (1.85) ($\rho = 1$; $a = 40.7$ Å; $b = 38.3$ Å; $c = 12.4$ Å; $M: 6281$; $N: 6.02 \times 10^{23}$).

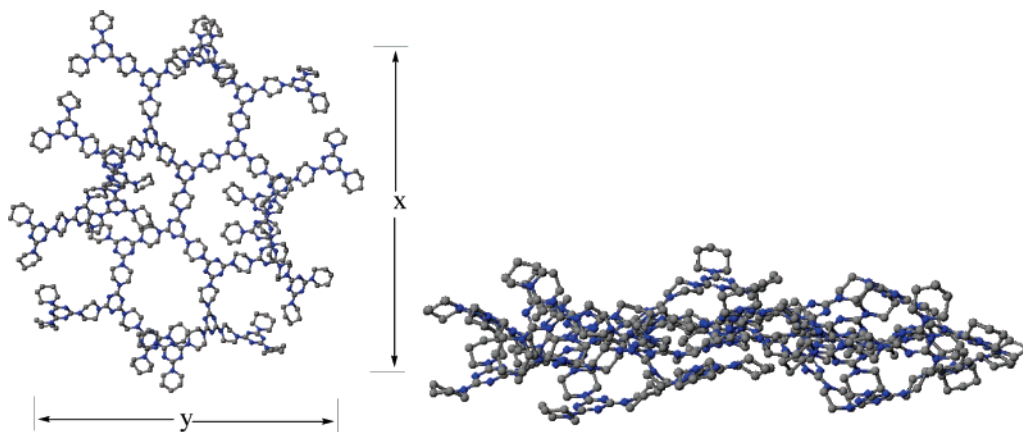


FIGURE 9. Optimized conformation of $G_4-N\sim N-G_4$ at gas phase by an MM2 model in CaChe program (left) and a side-view of $G_4-N\sim N-G_4$ (right) (hydrogens are omitted for clarity, C: gray, N: blue).

columns, and the more elliptical G_4-NH exhibits a rectangular columnar phase. A side view of the optimized structure shows that the core is not coplanar due to the repulsions between piperazine and triazine moieties (Figure 9, right). As the conformations of $G_4-N\sim N-G_4$ and G_4-NH based on the molecular mechanic simulation are not coplanar, this may explain why the layer-to-layer arrangement of dendron or dendrimer is not unambiguous, and consequently, the corresponding reflection of the XRD pattern is broad.

Conclusion

In addition to dendrons G_n-NH and G_n-Cl ($n = 2-4$) we further prepare new dendrimers, $G_n-N\sim N-G_n$ ($n = 2-4$) efficiently. It is noteworthy that the protecting and deprotecting processes are not needed during their preparation. By investigating a representative sample, they are transparent and possess good thermal stability. Interestingly, the mesogenic behaviors of the dendrimers and dendrons are versatile. Dendrimer $G_4-N\sim N-G_4$ shows a monotropic hexagonal columnar phase, and dendron G_4-NH shows a rectangular columnar phase during thermal processes. Although G_4-Cl shows a monotropic columnar phase in a narrow range, a coexisting crystalline phase was also observed accordingly.

Experimental Section

General Procedure for the Preparation of $G_n-N\sim N-G_n$ ($n = 2-4$). $G_2-N\sim N-G_2$: G_2-Cl (1.4 g, 1 mmole) and G_2-NH (1.45 g, 1 mmole) in THF (50 mL) were stirred at 70 °C for 20 h. KOH (0.56 g, 10 mmole) in water (50 mL) was added and then extracted with CH_2Cl_2 (2×40 mL). The combined organic extracts were further washed with aqueous solution (50 mL, pH = 10) and then water (2×50 mL) and were dried over magnesium sulfate. Solvent was removed at reduced pressure, and the extracts were then purified by chromatography on silica

to give $G_2-N\sim N-G_2$ in 72% yield (2.02 g). 1H NMR ($CDCl_3$) δ 0.88 (s, 48H, $J = 6.4$, $16 \times CH_3$), 1.23–1.30 (m, 160H, $80 \times CH_2$), 1.52–1.60 (m, 32H, $16 \times CH_2$), 3.45 (t, 32H, $J = 7.2$, $16 \times CH_2$), 3.79 (s, br, 40H, $20 \times CH_2$). ^{13}C NMR ($CDCl_3$) δ 14.14, 22.69, 27.17, 27.38, 28.15, 28.30, 29.31, 29.50, 29.68, 31.92, 43.14, 46.92, 47.18, 165.08, and 165.45. MS for $C_{166}H_{313}N_{36}$ ($M + H$) $^+$: Calcd 2813, Found 2813. EA: Calcd C, 70.89; H, 11.18; N, 17.93. Found C, 70.75; H, 11.20; N, 17.98.

$G_3-N\sim N-G_3$ and $G_4-N\sim N-G_4$ were prepared similarly.

$G_3-N\sim N-G_3$: 1H NMR ($CDCl_3$) δ 0.88 (t, 96H, $J = 6.4$, $32 \times CH_3$), 1.20–1.31 (m, 320H, $160 \times CH_2$), 1.50–1.62 (m, 64H, $32 \times CH_2$), 3.45 (s, br, 64H, $32 \times CH_2$), 3.75 (s, br, 104H, $52 \times CH_2$). ^{13}C NMR ($CDCl_3$) δ 14.14, 22.69, 27.16, 27.39, 28.15, 28.31, 29.31, 29.51, 29.69, 31.92, 43.16, 46.93, 47.22, 165.07 and 165.45. MS for $C_{350}H_{649}N_{84}$ ($M + H$) $^+$: Calcd. 6034, Found 6034. EA: Calcd. C 69.67; H 10.83; N 19.50, Found C 69.41; H 10.82; N 19.11%.

$G_4-N\sim N-G_4$: 1H NMR ($CDCl_3$) δ 0.88 (s, br, 192H, $64 \times CH_3$), 1.28 (s, br, 640H, $320 \times CH_2$), 1.58 (s, br, 128H, $64 \times CH_2$), 3.45 (s, br, 128H, $64 \times CH_2$), 3.81 (s, br, 232H, $116 \times CH_2$). ^{13}C NMR ($CDCl_3$) δ 14.15, 22.70, 27.17, 27.40, 28.16, 28.32, 29.32, 29.51, 29.70, 31.93, 43.17, 46.94, 47.22, 165.07, and 165.44. MS for $C_{718}H_{1321}N_{180}$ ($M + H$) $^+$: Calcd 12478.9, Found 12478.9. EA: Calcd C, 69.12; H, 10.65; N, 20.21. Found C, 68.72; H, 10.66; N, 19.91.

Acknowledgment. This work was financially supported by the National Chi Nan University and the National Science Council (NSC 95-2113-M-260-002).

Supporting Information Available: 1H and ^{13}C NMR spectra, general characterization method of dendrimers, and computational data of G_4-Cl , G_4-NH and $G_4-N\sim N-G_4$. This material is available free of charge via the Internet at <http://pubs.acs.org>.

JO701990W